Differential regulation of bile acid homeostasis by the farnesoid X receptor in liver and intestine

Insook Kim,* Sung-Hoon Ahn,* Takeshi Inagaki,† Mihwa Choi,† Shinji Ito,* Grace L. Guo,[1,*] Steven A. Kliewer,† and Frank J. Gonzalez[2,*]

Laboratory of Metabolism,* National Cancer Institute, National Institutes of Health, Bethesda, MD 20892; and University of Texas Southwestern Medical Center,† Dallas, TX 75390

Abstract Bile acid concentrations are controlled by a feedback regulatory pathway whereby activation of the farnesoid X receptor (FXR) represses transcription of both the CYP7A1 gene, encoding the rate-limiting enzyme in the classic bile acid synthesis pathway, and the CYP8B1 gene, required for synthesis of cholic acid. The tissue-specific roles of FXR were examined using liver- and intestine-specific FXR-null models. FXR deficiency in either liver ($Fxr^{\Delta L}$) or intestine ($Fxr^{\Delta IE}$) increased bile acid pool size. Treatment with the FXR-selective agonist GW4064 significantly repressed CYP7A1 in $Fxr^{\Delta L}$ mice but not $Fxr^{\Delta IE}$ mice, demonstrating that activation of FXR in intestine but not liver is required for short-term repression of CYP7A1 in liver. This intestinal-specific effect of FXR is likely mediated through induction of the hormone FGF15, which suppresses CYP7A1. In comparison to CYP7A1, FXR-mediated repression of CYP8B1 was more dependent on the presence of FXR in liver and less dependent on its presence in intestine. Consistent with these findings, recombinant FGF15 repressed CYP7A1 mRNA levels without affecting CYP8B1 expression. These data provide evidence that FXR-mediated repression of bile acid synthesis requires the complementary actions of FXR in both liver and intestine and reveal mechanistic differences in feedback repression of CYP7A1 and CYP8B1.—Kim, I., S-H. Ahn, T. Inagaki, M. Choi, S. Ito, G. L. Guo, S. A. Kliewer, and F. J. Gonzalez. **Differential regulation of bile acid homeostasis by the farnesoid X receptor in liver and intestine. *J. Lipid Res.* 2007.** 48: **2664–2672.**

Supplementary key words FXR • FGF15 • CYP7A1 • CYP8B1 • liver-specific FXR null mice • intestine-specific FXR null mice

Bile acids are amphiphilic end products of cholesterol catabolism that facilitate lipid absorption in the intestine. Bile acids are synthesized in the liver, released into the proximal intestine, and reabsorbed in the distal intestine (1). Release of bile from the gallbladder to the proximal intestine is induced by cholecystokinin, a hormone secreted from the duodenum in response to food intake (2). Conversely, gallbladder filling is regulated by the hormone FGF15, which is secreted from the ileum in response to bile acids (3). Disruption of bile acid homeostasis can cause cholestasis, diarrhea, and lipid malabsorption (4–7) and can affect lipid homeostasis by changing lipid absorption and altering the expression of genes that control lipid metabolism (8–11). In addition, owing to their cytotoxic, detergent-like properties, chronic exposure to elevated bile acids causes spontaneous liver tumor development in *Fxr*-null mice (12, 13). Bile acids also modulate liver regeneration (14) and energy expenditure (15).

The farnesoid X receptor (FXR) is a major bile acid sensor that protects the liver from bile acid toxicity by regulating the transcription of genes involved in bile acid homeostasis. Recently, the physiological ramifications of FXR have been expanded to include broader roles in glucose and lipid homeostasis (16–19). FXR is expressed in liver, intestine, kidney, and adrenal. Among the genes regulated by FXR are those encoding enzymes involved in bile acid synthesis, such as CYP7A1 and CYP8B1, and transport, such as BSEP and OSTα/β (20–25). The global *Fxr*-null mouse model has been a valuable model for investigating the roles of FXR in vivo (26). FXR-deficient mice fail to adapt to dietary cholic acid overload and exhibit dyslipidemia with elevated serum cholesterol and triglyceride concentrations (26, 27). The recent finding that FXR regulates transcription of the gene encoding the hormone FGF15/19 in intestine suggested a role for FXR in the cross-talk between intestine and liver. FGF15/19 cooperates with the orphan nuclear receptor SHP, whose expression is also regulated by FXR, to repress CYP7A1 and bile acid synthesis in liver (20, 28, 29). However, direct evaluation of the relative importance of FXR in liver and

Manuscript received 20 July 2007 and in revised form 22 August 2007.

Published, JLR Papers in Press, August 24, 2007.
DOI 10.1194/jlr.M700330-JLR200

Abbreviations: BW, body weight; CA, cholic acid; DCA, deoxycholic acid; FXR, farnesoid X receptor; LC-MS/MS, liquid chromatography tandem mass spectrometry; MCA, murocholic acid; RT-qPCR, real-time quantitative PCR; TCA, taurocholic acid; TDCA, taurodeoxycholic acid.

[1] Present address of G. L. Guo: University of Kansas Medical Center, Kansas City, KS 66160.

[2] To whom correspondence should be addressed.
e-mail: fjgonz@helix.nih.gov

intestine in regulating bile acid homeostasis has not been possible owing to the lack of tissue-specific *Fxr*-null mice. In this report, we provide the first characterization and comparison of liver- and intestine-specific *Fxr*-null mice. Our results demonstrate that FXR in intestine is crucial for feedback regulation of bile acid synthesis in liver. Furthermore, they reveal unexpected differences in the mechanisms whereby FXR represses CYP7A1 and CYP8B1.

MATERIALS AND METHODS

Generation of liver-specific and intestine-specific *Fxr*-null mice

Generation of global *Fxr*-null mice (26) and FGF15-null mice (29) was previously described, and the background matched wild-type animals used as controls. To generate liver-specific *Fxr*-null mice ($Fxr^{\Delta L}$) and intestine-specific *Fxr*-null mice ($Fxr^{\Delta IE}$), homozygous *Fxr*-floxed mice ($Fxr^{fl/fl}$) (26) were crossed with mice harboring the cre-recombinase under the control of the albumin promoter [Alb-Cre mice, from Derek LeRoith (30)] and villin promoter [Villin-Cre mice, from Deborah Gumucio (31)], respectively. Animals were maintained on a C57B/6;129 mixed background. For genotyping, 50 ng of tail DNA was amplified in a 10 μl final reaction mixture containing 1.5 mM $MgCl_2$, 0.25 mM deoxynucleotide triphosphates, 2.5% Me_2SO, 0.25 U *taq*-polymerase, 0.2 μM FXR-geno-F (5′-atagacaaccccagtgaccc-3′), and 0.2 μM FXR-geno-R (5′-tctaaaggatagccgaatct-3′). Cycling conditions were 94°C for 3 min and then 30 cycles at 94°C for 30 s, 60°C for 30 s, and 72°C for 30 s, followed by a 10 min extension at 72°C. These primers yield products of 300 bp and 380 bp for the wild-type and the $Fxr^{fl/fl}$ alleles, respectively. Genotyping for cre-transgene was performed as previously described using microsomal epoxide hydrolase as an internal control (32). Disruption of *Fxr* was quantified by real-time quantitative PCR (RT-qPCR) using primers designed against the deleted exon: forward 5′-cacagcgatcgtcatcctctct-3′ and reverse 5′-tctcaggctggtacatcttgca-3′. Mice were maintained under a standard 12 h light/12 h dark cycle with water and chow provided ad libitum. Animal handling was in accordance with animal study protocols approved by the National Cancer Institute Animal Care and Use Committee.

Animal treatment

All the experiments were performed with age-matched 8 to 10 week-old male mice, and $Fxr^{fl/fl}$ littermates without albumin-cre recombinase transgene or villin-cre recombinase transgene were used as controls to $Fxr^{\Delta L}$ mice and $Fxr^{\Delta IE}$ mice, respectively.

GW4064 treatment. Mice received a first dose of GW4064 (100 mg/kg in 1% Tween 80/1% methylcellulose) or vehicle by oral gavage followed by a second dose 12 h later and were killed 2 h later for tissue collection. Tissues were flash-frozen in liquid nitrogen and stored at −80°C until RNA was prepared. Small and large intestines were removed and flushed with ice cold phosphate-buffered saline. Small intestine was divided into three equal lengths designated duodenum (proximal), jejunum (medial), and ileum (distal). The three segments were cut open longitudinally, and the mucosa was gently scraped and flash-frozen in liquid nitrogen.

Recombinant FGF15 treatment. Wild-type mice (C57B6, male) were treated with saline control or 100 μg/kg recombinant FGF15 by tail vein injection and euthanized for tissue collection 1 h later. Recombinant FGF15 was expressed by infection of human embryonic retinoblast 911 cells with an FGF15-expressing adenovirus and purified from the media as previously described (29).

Serum chemistry

Serum was prepared by centrifugation at 8,000 rpm for 10 min in a serum separator, and serum triglyceride and total cholesterol were analyzed by using colorimetric assay kits, Infinity triglyceride assay reagent and cholesterol liquid stable reagents (Thermo Electronics, Inc.; Melbourne, Australia), respectively. Total bile acids in serum were analyzed by colorimetric enzyme assay using a bile acid kit (Trinity Biotech; St. Louis, MO).

Gene expression analysis

Northern blot analysis. Total RNA was extracted using Trizol® (Invitrogen; Carlsbad, CA) following the manufacturer's protocol. RNA (10 μg) was separated on 1% formaldehyde-agarose gels and transferred to GeneScreen Plus membranes (Dupont; Wilmington, DE) overnight. The blots were hybridized at 62°C in PerfectHyb plus solution (Sigma) with random primer-labeled cDNA probes and exposed to a phosphorimager screen cassette and visualized using the Storm 860 PhosphorImager system (Amersham Biosciences).

RT-qPCR. qPCR was performed using cDNA generated from 1 μg total mRNA with the SuperScript III Reverse Transcriptase kit (Invitrogen). Primers were designed for qPCR using the Primer Express software (Applied Biosystems; Foster City, CA) based on GenBank sequence data (CYP7A1: forward 5′-agcaactaaacaacctgccagtacta-3′, reverse 5′-gtccggatattcaaggatgca-3′; FGF15: forward 5′-gaggaccaaaacgaacgaaatt-3′, reverse 5′-acgtccttgatggcaatcg-3′; SHP: forward 5′-cgatcctcttcaacccagatg-3′, reverse 5′-agggctccaagacttcacaca-3′; BSEP: forward 5′-acagaagcaaagggtagccatc-3′, reverse 5′-ccatttgtgatttacaaacattcca-3′; IBABP: forward 5′-ggtcttccaggagacgtgat-3′, reverse 5′-acattctttgccaatggtga-3′; paraoxonase 1: forward 5′-tgggtctgtcgtggtccaat-3′, reverse 5′-atcaagggaaatgccaatgc-3′; CYP8B1: forward 5′-acgcttcctctatcgcctgaa-3′, reverse 5′-gtg cctcagacgcagaggat-3′; OSTα: forward 5′-atgcatctgggtgaacagaa-3′, reverse 5′-gagtagggaggtgagcaagc-3′; OSTβ: forward 5′-gaccacagtgcagagaaagc-3′, reverse 5′-cttgtcatgaccaccaggac-3′; and β-actin: forward 5′-tattggcaacgagcggttcc-3′, reverse 5′-ggcatagaggtctttacggatgtc-3′). RT-qPCR reactions contained 25 ng of cDNA, 150 nM of each primer, and 5 μl of SYBR Green PCR Master Mix (Applied Biosystems) in a total volume of 10 μl. All reactions were performed in triplicate on an Applied Biosystems Prism 7900HT sequence detection system, and relative mRNA levels were calculated by the comparative threshold cycle method using β-actin as the internal control.

Liquid chromatography tandem mass spectrometry analysis of conjugated bile acids in the bile acid pool and free bile acids in fecal extracts

To determine the bile acid pool size, liver, gallbladder, and small intestine with its contents were removed from 4 h-fasted mice, weighed and freeze-dried overnight. Fecal excretion of bile acid was determined in stools collected over 24 h in metabolic cages. Collected stools were air-dried over 48 h. Dried bile acid pool and stool samples were powdered; bile acids were extracted in 5 ml of 70% ethanol at 55°C for 4 h, and bile salts species were analyzed by liquid chromatography tandem mass spectrometry (LC-MS/MS) performed on a PESCIEX API200 ESI triple-quadrupole mass spectrometer (PerkinElmer Life Sciences) controlled by Analyst software, as described previously

(33). Briefly, 200 μl of acetonitrile and an internal standard, 50 μl of dehydrocholic acid (20 μM in methanol), were added to 100 μl alcoholic extract of bile acids from bile acid pool or stools, and the mixture was centrifuged at 14,000 *g* for 5 min. Bile acids were further solid-phase extracted and eluted by 100% methanol using Sepak®, and then the organic solvent was evaporated by Speed-Vac (Thermo Savant, Waltham, MA). The residue was reconstituted in 60 μl of 0.1% formic acid in 50% methanol. Final extract (10 μl) was injected to LC-MS/MS and separated on the mobile phase of 0.1% formic acid in acetonitrile-water-ethanol (25:50:20).

Statistical analysis

Data are presented as mean ± standard deviation unless described otherwise, and statistical significance was analyzed by Student's *t*-test.

RESULTS

Tissue-specific deletion of FXR in liver or intestinal epithelium

Liver-specific or intestinal epithelium-specific disruption of *Fxr* expression was examined by Northern blot analysis (**Fig. 1A, B**). In $Fxr^{\Delta L}$ mice harboring the homozygous floxed *Fxr* allele with the albumin-cre recombinase transgene, FXR mRNA was undetectable in liver but expression of FXR mRNA in ileal mucosa was comparable to that in $Fxr^{fl/fl}$ mice. On the other hand, in $Fxr^{\Delta IE}$ mice harboring the homozygous floxed *Fxr* allele and the villin-cre recombinase transgene, the expression of FXR in the epithelium of the intestinal tract (including duodenum, jejunum, ileum, and colon) was significantly lower than in $Fxr^{fl/fl}$ mice, and its expression in liver and kidney was comparable to that of $Fxr^{fl/fl}$ mice (Fig. 1C). The $Fxr^{\Delta L}$ or $Fxr^{\Delta IE}$ mice are viable and display no overt abnormalities.

The whole-body *Fxr*-null mice exhibit dyslipidemia with elevated triglyceride, cholesterol, and bile acid levels (**Fig. 2A**) (26). In contrast, total serum bile acid levels in $Fxr^{\Delta L}$ and $Fxr^{\Delta IE}$ mice were not significantly different compared with controls (Fig. 2A). As in the case of the *Fxr*-null mice, serum triglyceride and cholesterol levels of $Fxr^{\Delta L}$ were significantly elevated compared with littermate controls, whereas serum lipid levels of $Fxr^{\Delta IE}$ were not significantly different from littermate controls (Fig. 2B, C). These data indicate that the presence of FXR in either liver or intestine is sufficient to maintain normal serum bile acid concentrations but that FXR in liver is required for controlling serum triglyceride and cholesterol levels.

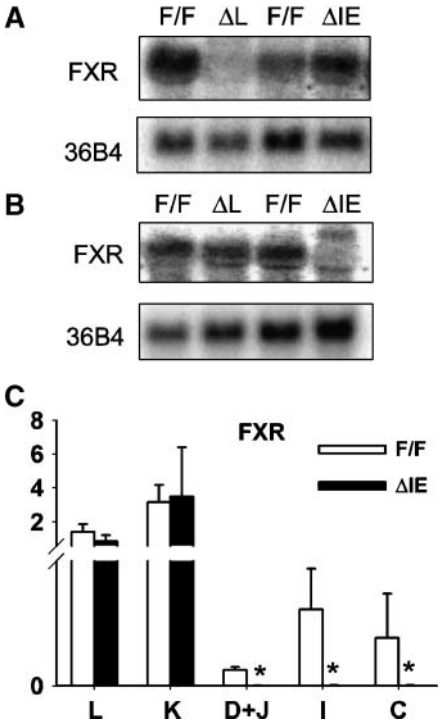

Fig. 1. Tissue-specific disrupition of farnesoid X receptor (FXR) expression in liver-specific and intestinal-specific FXR-null mouse. Total RNA from (A) livers or (B) ileal mucosa of liver-specific and intestine-specific FXR-null mice and littermate controls was extracted and subjected to Northern blot analysis. C: Real-time quantitative PCR (RT-qPCR) analysis of FXR expression in the $Fxr^{\Delta IE}$ mouse model. L, liver; K, kidney; D, duodenum; J, jejunum; I, ileum; C, colon; F/F, homozygous floxed FXR littermate controls; ΔL, $Fxr^{fl/fl}$, albumin-cre+; ΔIE, $Fxr^{fl/fl}$, villin-cre+; n = 3. Error bars indicate ± SD. * $P < 0.05$.

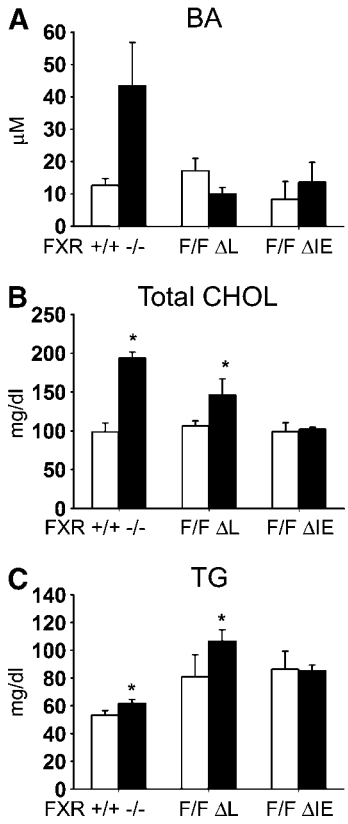

Fig. 2. Serum chemistry of *Fxr*-null, $Fxr^{\Delta L}$, and $Fxr^{\Delta IE}$ mice. Serum samples from 4 h-fasted animals were analyzed for (A) total bile acids, (B) cholesterol, and (C) triglyceride. BA, bile acids; CHOL, cholesterol; TG, triglycerides; F/F: homozygous floxed FXR littermate controls; ΔL, $Fxr^{fl/fl}$, albumin-cre+; ΔIE, $Fxr^{fl/fl}$, villin-cre+; n = 5–6. Error bars indicate ± SD. * $P < 0.05$.

Bile acid composition in the bile acid pool and feces

It was previously shown that the total bile acid pool size is increased in *Fxr*-null mice (12, 34). To investigate the relative contribution of FXR in liver and intestine to maintaining the bile acid pool size, alcohol extracts of total bile acids were prepared from liver, gallbladder, and small intestine and analyzed for both total bile acid levels and bile acid species by LC-MS/MS. Consistent with previous reports, the total bile acid pool size was increased in *Fxr*-null mice (**Fig. 3A**). A significant increase in the bile acid pool size was also observed in $Fxr^{\Delta L}$ mice. Although a trend toward increased total bile acid pool size was seen in $Fxr^{\Delta IE}$ mice (Fig. 3A), this difference did not achieve statistical significance. The magnitude of the increase was greater in the *Fxr*-null mice than in either the $Fxr^{\Delta L}$ or $Fxr^{\Delta IE}$ mice, suggesting that FXR in both liver and intestine contributes to controlling the overall bile acid pool size.

To determine the contribution of different pathways to the increased bile acid pool size, individual bile acid species were analyzed in more detail. In our initial analysis of free-form bile acids, including cholic acid (CA), murocholic acid (αMCA), βMCA, and deoxycholic acid (DCA), the combined free bile acid level was less than 10% of the bile acid pool, and no significant differences between controls and *Fxr*-null models were observed. Briefly, the combined free bile acid level in the bile acid pool was 2.6 ± 0.9 and 3.8 ± 0.9 μmol/100 g body weight (BW) in wild-type and *Fxr*-null mice, respectively; 3.9 ± 1.4 and 4.5 ± 2.0 μmol/100 g BW in controls and $Fxr^{\Delta L}$ mice, respectively; and 2.3 ± 1.6 and 2.6 ± 1.3 μmol/100 g BW in controls and $Fxr^{\Delta IE}$ mice, respectively. Because most bile acids are present in their conjugated forms (1), only the conjugated bile acids were analyzed. There was a significant increase in taurocholic acid (TCA), the most abundant bile acid, in *Fxr*-null, $Fxr^{\Delta L}$, and $Fxr^{\Delta IE}$ groups compared with their controls (Fig. 3B–D). TCA levels increased 2.6-, 1.4-, and 1.2-fold in *Fxr*-null, $Fxr^{\Delta L}$, and $Fxr^{\Delta IE}$ mice, respectively, compared with control mice. The relative magnitude of these changes is in good agreement with the overall changes in the bile acid pool size (Fig. 3A). The cholate derivative, taurodeoxycholic acid (TDCA), was also increased in all three null groups (Fig. 3B–D). In contrast, the second most abundant species, tauro-β-muricholic acid (TβMCA), was not significantly different in *Fxr*-null and $Fxr^{\Delta L}$ mice and was slightly decreased in $Fxr^{\Delta IE}$ mice compared with their controls. No significant difference was detected in taurochenodeoxycholic acid (TCDCA) levels in all three null groups (Fig. 3B–D). These results indicate that the increase in bile acid pool size in the *Fxr*-deficient models is due specifically to an increase in cholate and its derivatives.

During enterohepatic circulation, a small fraction of bile acids are lost in the stool, whereas the vast majority of bile acids are reabsorbed in the ileum (1). Bile acid composition was analyzed in fecal extracts to determine whether the increased bile acid pool size was reflected in fecal bile acid excretion (**Fig. 4A–C**). As expected, the fecal bile acids were almost exclusively unconjugated, owing to the actions of gut microflora (data not shown). Interestingly, DCA was significantly increased in fecal extracts from $Fxr^{\Delta IE}$ mice but not from *Fxr*-null or $Fxr^{\Delta L}$ mice. Although there was a trend toward increased fecal CA in *Fxr*-null, $Fxr^{\Delta l}$, and $Fxr^{\Delta IE}$ mice compared with their controls, there were no other significant changes in fecal bile acid concentrations.

Gene expression analysis

To investigate the mechanistic basis for the increased bile acid pool size in $Fxr^{\Delta L}$ and $Fxr^{\Delta IE}$ mice, gene expression was analyzed by qPCR using total RNA from liver and ileal mucosa of $Fxr^{\Delta L}$ and $Fxr^{\Delta IE}$ mice. Similar to previous findings in *Fxr*-null mice, the basal level of CYP7A1

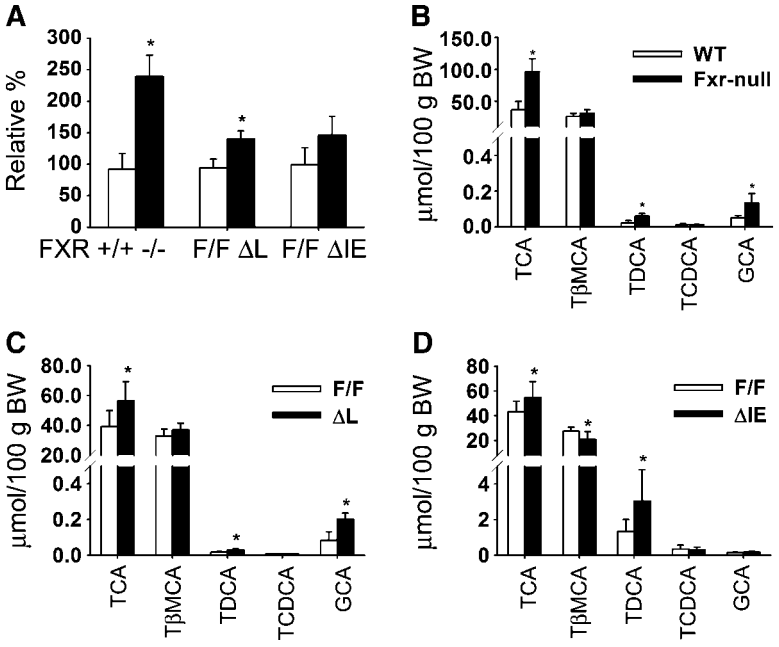

Fig. 3. Liquid chromatography tandem mass spectrometry (LC-MS/MS) analysis of conjugated bile acids in bile acid pool. Total bile acids were extracted from freeze-dried bile acid pool composed of liver, gallbladder, and small intestine with its contents and analyzed for conjugated bile acids as described in MATERIALS AND METHODS. A: Total bile acid pool (% control). Individual bile acids: global *Fxr*-null (n = 4–5) (B); liver-specific FXR-null (ΔL) (n = 4–5) (C); and intestine-specific *Fxr*-null (ΔIE) (n = 9–10) (D); BW, body weight; F/F, homozygous floxed FXR littermate controls; TCA, taurocholic acid; TβMCA, tauro-β-muricholic acid; TDCA, taurodeoxycholic acid; TCDCA, taurochenodeoxycholic acid; GCA, glycocholic acid.

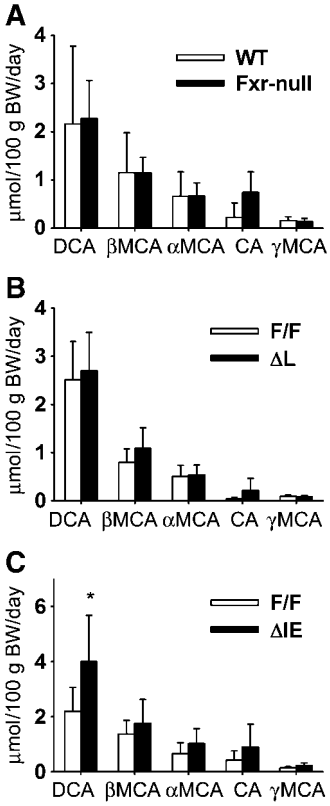

Fig. 4. LC-MS/MS analysis of free bile acids in fecal extracts. Total bile acids were extracted from air-dried feces collected over 24 h and analyzed for free bile acids. Fecal extracts of *Fxr*-null (n = 4) (A), liver-specific *Fxr*-null (ΔL) (n = 5) (B), and intestine-specific *Fxr*-null (ΔIE) (n = 8) (C). DCA, deoxycholic acid; MCA, muricholic acid; CA, cholic acid; WT, wild-type; F/F, homozygous floxed FXR littermate controls.

mRNA expression was significantly increased in $Fxr^{\Delta L}$ mouse livers (**Fig. 5**). Surprisingly, no change in basal CYP7A1 levels was seen in $Fxr^{\Delta IE}$ mice (**Fig. 6**). There was no significant change in basal CYP8B1 mRNA levels in either the $Fxr^{\Delta L}$ or $Fxr^{\Delta IE}$ mice (Figs. 5, 6). There was a trend toward decreased basal SHP expression in liver but not ileum of $Fxr^{\Delta L}$ mice; conversely, there was a trend toward decreased SHP expression in ileum but not liver of $Fxr^{\Delta IE}$ mice. IBABP mRNA levels were significantly lower in ileum of $Fxr^{\Delta IE}$ mice (Fig. 6).

To further examine the role of FXR in regulating gene expression in liver and intestine, $Fxr^{\Delta L}$, $Fxr^{\Delta IE}$, and control mice were administered either the FXR-selective synthetic agonist GW4064 or vehicle. As expected, GW4064 induced SHP and BSEP mRNA expression in livers of control mice but not $Fxr^{\Delta L}$ mice (Fig. 5) and induced IBABP, OSTα, and OSTβ in ileum of control mice but not $Fxr^{\Delta IE}$ mice (Fig. 6). Interestingly, in $Fxr^{\Delta L}$ mouse livers, CYP7A1 mRNA expression was markedly repressed by GW4064. In contrast, GW4064 did not significantly repress CYP7A1 in $Fxr^{\Delta IE}$ mice, whereas BSEP expression was induced consistently in $Fxr^{\Delta IE}$ mice (Fig. 6). Taken together, these data show that FXR in intestine but not liver is required for acute repression of CYP7A1.

Unexpectedly, CYP8B1 showed a completely different pattern of regulation compared with CYP7A1. Although GW4064 treatment repressed CYP8B1 expression >5-fold in livers of control mice, repression was reduced to <2-fold in $Fxr^{\Delta L}$ mice (Fig. 5). In marked contrast to CYP7A1, deletion of FXR in intestine had only a modest effect on GW4064-mediated repression of CYP8B1 (Fig. 6). These data demonstrate that CYP7A1 and CYP8B1 are differentially regulated by FXR, with CYP7A1 repression more dependent on FXR in intestine and CYP8B1 repression more dependent on FXR in liver.

The demonstration that intestinal FXR is required for efficient repression of CYP7A1 is consistent with the FXR-FGF15 enterohepatic signaling cascade playing a prominent role in CYP7A1 regulation. FGF15 was not induced by GW4064 in ileum of $Fxr^{\Delta IE}$ mice but was induced in ileum of control and $Fxr^{\Delta L}$ mice (Figs. 5, 6). The potential role of the FXR-FGF15 signaling cascade in regulating gene expression was further investigated by analyzing the hepatic expression of paraoxonase 1 (PON1), which is regulated by FGF15 (35, 36). PON1 mRNA levels were significantly reduced by GW4064 in control and $Fxr^{\Delta L}$ mouse liver but not in liver of $Fxr^{\Delta IE}$ mice (Figs. 5, 6). These data provide additional evidence that FGF15 originating from the small intestine contributes to the regulation of hepatic genes in response to GW4064 in FXR-deficient liver.

Differential effects of FGF15 on CYP7A1 and CYP8B1

To test directly whether FGF15 has differential effects on CYP7A1 and CYP8B1, wild-type mice were injected with recombinant FGF15 or saline control. The regulation of CYP7A1 by FGF15 and in *Fgf15*-null mice was consistent with previous observations (29). Notably, FGF15 efficiently repressed CYP7A1 expression but did not significantly affect CYP8B1 mRNA levels (**Fig. 7A**). To complement these studies, the effect of GW4064 administration on CYP7A1 and CYP8B1 expression was evaluated in wild-type and *Fgf15*-null mice. Whereas basal CYP7A1 mRNA levels were increased 3.5-fold in *Fgf15*-null mice, CYP8B1 mRNA levels were elevated a more modest 1.7-fold (Fig. 7B). As expected, GW4064 treatment repressed both CYP7A1 and CYP8B1 expression to a comparable degree in wild-type mice. However, in *Fgf15*-null mice, GW4064 repressed CYP8B1 expression but did not cause a significant decrease in CYP7A1 mRNA levels. Taken together, these data demonstrate that feedback repression of CYP7A1 is more strongly regulated by the FXR-FGF15 signaling cascade than is CYP8B1.

DISCUSSION

The regulation of bile acid homeostasis by FXR is an area of intense interest. In liver, FXR regulates a program of genes including CYP7A1, CYP8B1, SHP, and BSEP that impact bile acid pool size and composition. Likewise, in intestine, FXR regulates genes involved in bile acid homeostasis, including IBABP, ASBT, OSTα/β, and FGF15

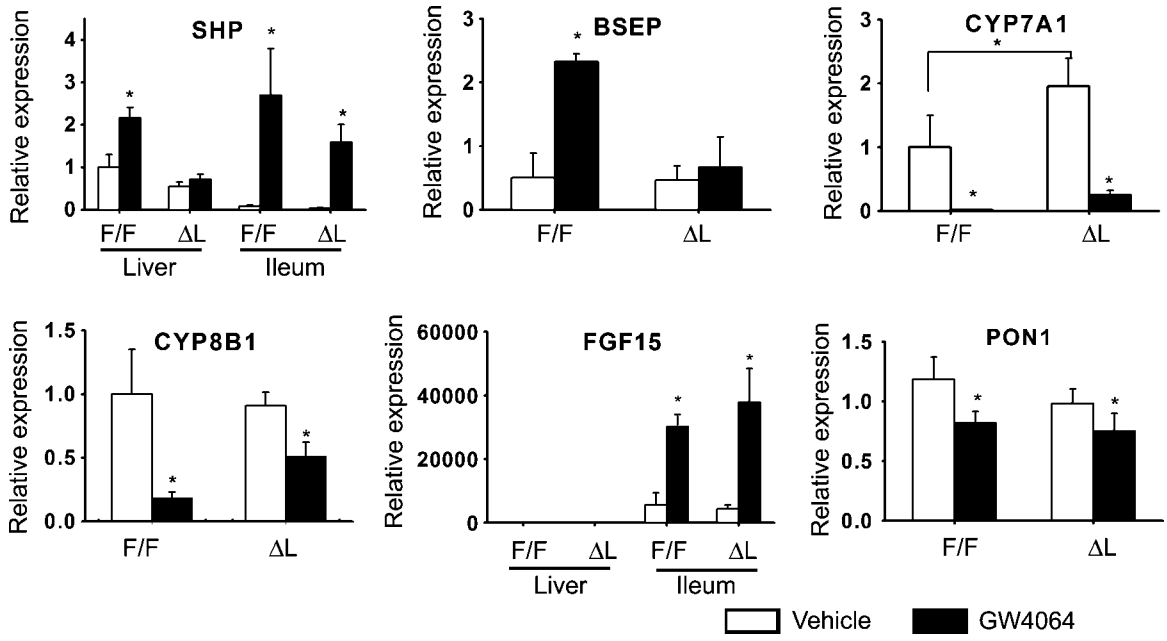

Fig. 5. Gene expression induced by GW4064 treatment in the liver-specific *Fxr*-null mice. Real-time quantitative PCR (RT-qPCR) analysis was performed on cDNA prepared from total RNA of liver or ileal mucosa of $Fxr^{fl/fl}$ littermate controls (F/F) or liver-specific *Fxr*-null (ΔL) treated with vehicle (open bars) or 100 mg/kg GW4064 (closed bars) by oral gavage as described in MATERIALS AND METHODS. CYP7A1, CYP8B1, BSEP, and PON1 expression was analyzed in liver. Data were presented as a relative value to the expression level of control treated with vehicle (n = 4–5; * $P < 0.05$ versus control treatment group). SHP, small heteromer partner; FGF15, fibroblast growth factor 15; BSEP, bile salts export pump; PON1, paraoxonase1. Error bars indicate ± SD.

(20–25). Although the whole-body knockout of FXR in mice causes marked changes in bile acid homeostasis (26, 27), its relative importance in liver and intestine was not known. In the current study, this question was systematically investigated using liver- and intestine-specific FXR-null mice.

These studies reveal that FXR in both liver and intestine makes important contributions to the regulation of bile acid homeostasis. Although the elimination of FXR in either liver or intestine caused increases in the bile acid pool size, including TCA and TDCA, these increases were not as pronounced as those seen in the *Fxr*-null mice. Moreover, whole-body deletion of FXR caused a significant increase in serum bile acid concentrations (26) that was not seen in either the $Fxr^{\Delta L}$ or $Fxr^{\Delta IE}$ mice. Taken together, these data demonstrate additive effects of FXR in liver and intestine under normal dietary conditions.

Notably, fecal DCA excretion, which is usually proportional to cholate pool size, was increased only in $Fxr^{\Delta IE}$ but not in *Fxr*-null and $Fxr^{\Delta L}$ mice. CA excretion tended to be higher in *Fxr*-null and $Fxr^{\Delta L}$ mice compared with controls but did not achieve statistical significance. Despite increased bile acid synthesis in *Fxr*-null mice, bile acid release to small intestine was not increased but was decreased (26) or comparable (27). The findings that fecal bile acid excretion is not altered in either *Fxr*-null or $Fxr^{\Delta L}$ mice and is increased in $Fxr^{\Delta IE}$ mice suggest that the increased bile acid pool size in $Fxr^{\Delta IE}$ mice is probably due to deregulation of bile acid synthesis rather than to an increase in bile acid reabsorption. Nevertheless, we cannot exclude the possibility of the contribution of deregulation of the bile salts transporter OSTα/β to the increased fecal bile acid excretion in $Fxr^{\Delta IE}$ mice. The effect of the selective FXR agonist GW4064 in liver- and intestine-specific FXR-null mice was also compared. As expected, SHP and BSEP were induced by GW4064 in the livers of $Fxr^{\Delta IE}$ but not $Fxr^{\Delta L}$ mice. Conversely, IBABP, SHP, and FGF15 were induced by GW4064 in small intestine of $Fxr^{\Delta L}$ but not $Fxr^{\Delta IE}$ mice. It was previously shown that FXR represses CYP7A1 through the coordinate induction of FGF15 in intestine (29) and SHP in liver (20, 21). FGF15 and SHP then act cooperatively to repress CYP7A1 transcription through a mechanism that is not yet understood. Although mice completely devoid of either FGF15 or SHP have markedly elevated basal CYP7A1 expression (29, 37), the relative contribution of intestinal and liver FXR to the repression of CYP7A1 was not known. The loss of significant repression of CYP7A1 in $Fxr^{\Delta IE}$ mice treated with GW4064 provides the first direct evidence that FXR in the gut regulates bile acid synthesis in the liver. The coincident loss of FGF15 induction suggests that this hormone is responsible for signaling from intestine to liver. Consistent with this possibility, FXR-mediated repression of PON1, which is also suppressed by FGF15 (35, 36), was lost in $Fxr^{\Delta IE}$ but not $Fxr^{\Delta L}$ mice. Notably, FXR-mediated repression of CYP7A1 was largely intact in the $Fxr^{\Delta L}$ mice despite the lack of hepatic SHP induction. These data demonstrate that induction of SHP above basal levels is not essential for FXR-mediated repression of CYP7A1.

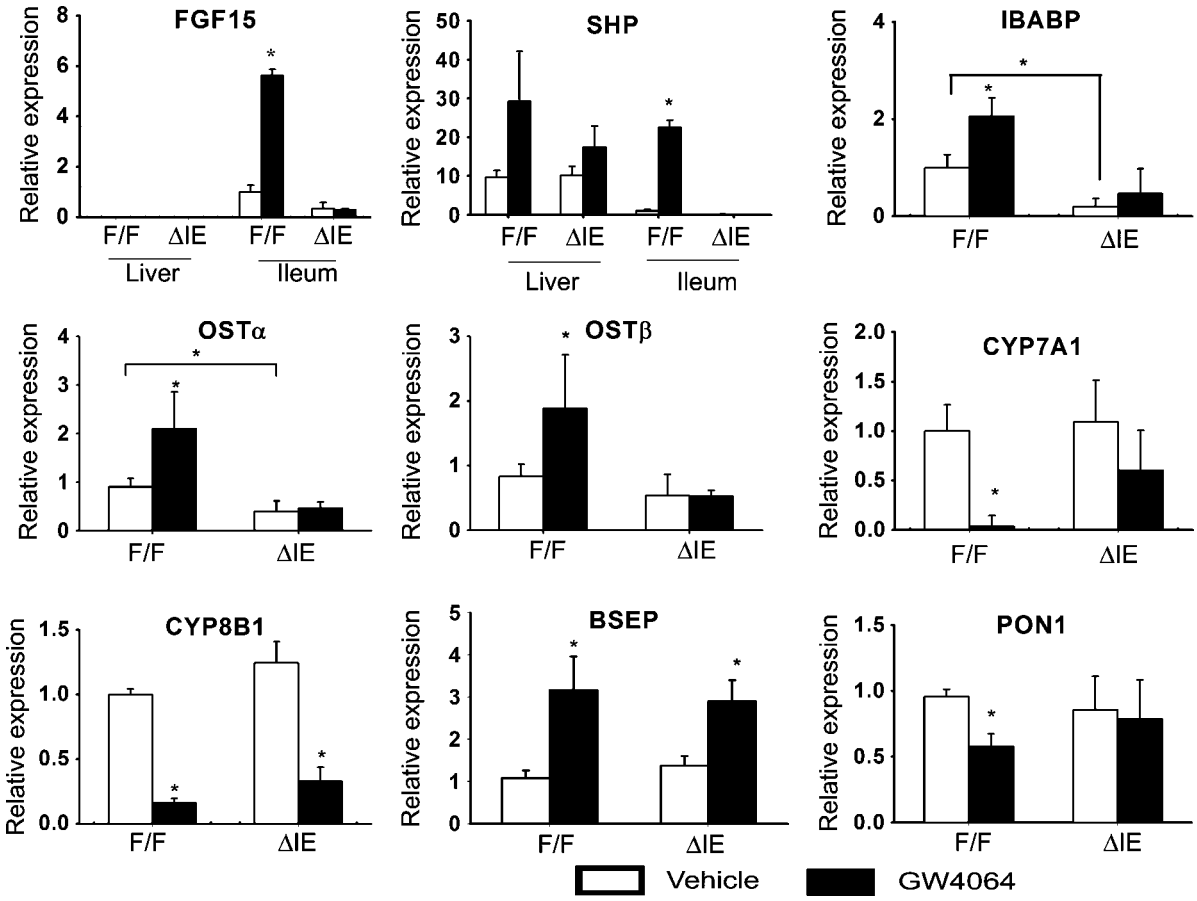

Fig. 6. Gene expression by GW4064 treatment in the intestine-specific FXR-null mice. RT-qPCR analysis was performed on total RNA from livers or ileal mucosa of $Fxr^{fl/fl}$ littermate controls (F/F) or intestine-specific *Fxr*-null (ΔIE) mice treated with vehicle (open bar) or GW4064 (closed bar) as described in MATERIALS AND METHODS. IBABP, OSTα, and OSTβ expression was analyzed in ileal mucosa. CYP7A1, CYP8B1, BSEP, and PON1 expression was analyzed in liver. Data are presented as a relative value to the expression level of control treated with vehicle (n = 4–5; * $P < 0.05$ versus control treatment group). Error bars indicate ± SD.

They further suggest that most of the acute effect of FXR on CYP7A1 transcription is mediated by induction of FGF15 in intestine.

There are several caveats that must be kept in mind when interpreting the CYP7A1 data from these studies. First, if intestinal FGF15 regulates CYP7A1, why do the $Fxr^{\Delta L}$ but not the $Fxr^{\Delta IE}$ mice have increased basal CYP7A1 mRNA levels? The regulation of CYP7a1 via intestinal FXR-FGF15 is presumably very cyclical, such that under normal physiological conditions, the bile acid flux to the distal small intestine at the end of the enterohepatic circulation would activate FXR in the ileum and then send signals to the liver for CYP7a1 repression. Thus, it is possible not to see a basal level induction of CYP7a1 in the liver of $Fxr^{\Delta IE}$ mice, especially when liver FXR and other transcription factors are intact. Nonetheless, deregulation of CYP7a1 in $Fxr^{\Delta IE}$ mice, which we demonstrated using a synthetic FXR agonist, may contribute to a trend toward increasing bile acid pool size. In addition, it is important to note that unlike the *Fgf15*-null mice, the $Fxr^{\Delta IE}$ mice still express FGF15, albeit at reduced levels, in the ileum. This residual FGF15 may be adequate to constrain CYP7A1 transcription in the context of an intact FXR response in liver. On the other hand, as with all gene knockout mice, it is also possible that the $Fxr^{\Delta IE}$ mice have undergone a long-term, compensatory response that constrains CYP7A1 expression even in the absence of the normal contribution of intestinal FXR to the regulation of bile acid synthesis. A related point is why the intestine-specific FXR-null mice show a trend toward an increased bile acid pool size even if they do not have increased basal CYP7A1 expression. One possibility is that the alternative pathway for bile acid synthesis is upregulated in the intestine FXR-null mice. However, according to the bile acid species analysis, a trend toward increasing bile acid pool size in $Fxr^{\Delta IE}$ mice is attributed mainly to an increase in cholate pool (taurocholate); thus, we hypothesized that an increase in bile acid pool size is due more to the classic (neutral) pathway than to the alternative pathway. Moreover, we did not observe an increase in muricholates or chenodeoxycholate, which are the main products of the acidic pathway in $Fxr^{\Delta IE}$ mice, compared with controls. At this point, the molecular basis for this trend is not known. A final caveat relates to the FXR-selective agonist,

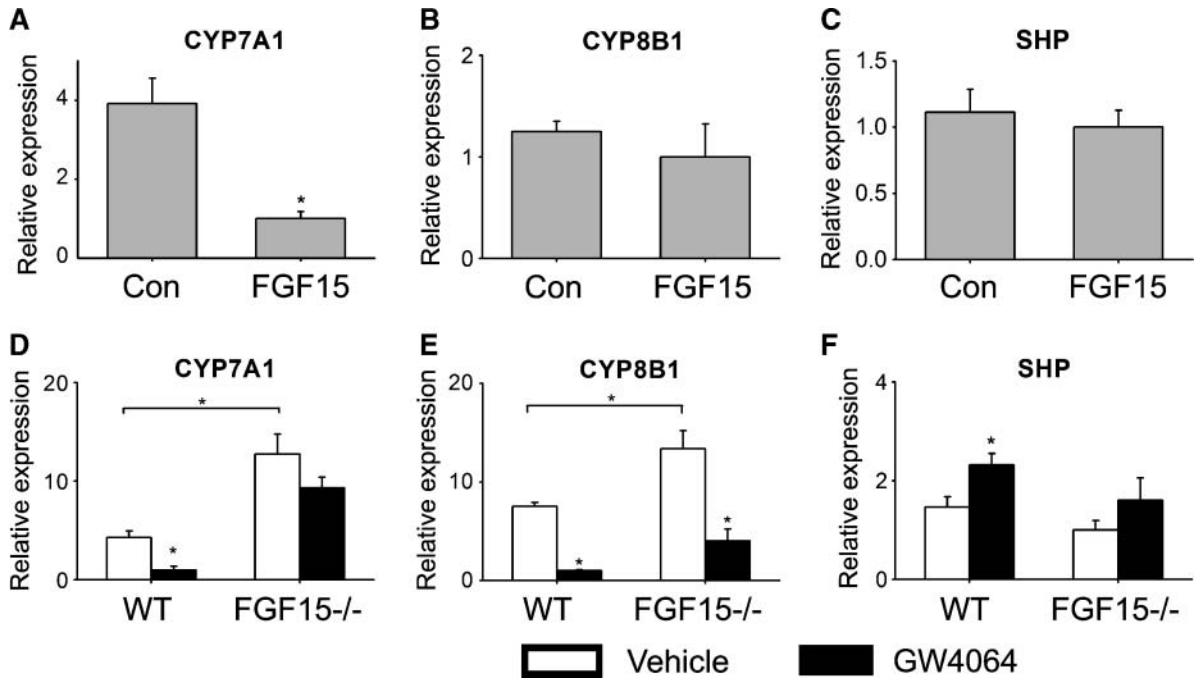

Fig. 7. Hepatic gene expression by recombinant FGF15 treatment in wild-type mice and GW4064 treatment in the *Fgf15*-null mice. RT-qPCR analysis was performed on total RNA from livers of wild-type mice injected with recombinant FGF15 or saline and euthanized 1 h later (A–C) (n = 3), and *Fgf15*-null and wild-type control mice treated with vehicle (open bars) or GW4064 (closed bars) and euthanized 14 h later (D–F) (n = 4–5). Mean ± SEM; * $P < 0.05$ versus control treatment group.

GW4064, which has poor bioavailability. Although the presence of GW4064 in liver is evidenced by the induction of BSEP in controls and $Fxr^{\Delta IE}$ mice, we cannot exclude the possibility of more-pronounced effects on FXR activity in intestine than liver due to the poor bioavailability of GW4064. This relative lack of efficacy in liver could potentially lead to an underestimation of the importance of FXR-mediated induction of SHP and possibly other genes in liver in the feedback regulation of CYP7A1.

FXR also plays an important role in the feedback repression of CYP8B1. An unexpected outcome of our studies was the differential regulation of CYP7A1 and CYP8B1 by FXR. Whereas FXR-induced repression of CYP7A1 was more strongly affected by disruption of FXR in intestine, repression of CYP8B1 was more sensitive to loss of FXR in liver. One interpretation of these data is that CYP7A1 is regulated more strongly by the FXR-FGF15 pathway in intestine and CYP8B1 is more sensitive to repression via FXR activation in liver. In support of this hypothesis, CYP7A1 was efficiently repressed by injection of FGF15, whereas CYP8B1 was not. Moreover, CYP8B1 was repressed by FXR activation in *Fgf15*-null mice, whereas CYP7A1 was not. Finally, whereas basal expression of CYP7A1 increased 3-fold in *Fgf15*-null mice, CYP8B1 mRNA levels increased less than 2-fold. Regarding this latter point, it must be noted that CYP8B1 mRNA levels were significantly increased in the *Fgf15*-null mice, indicating that CYP8B1 expression is affected by FGF15, at least in the long term.

It was previously shown that treatment of humans with the bile acid sequestrant cholestyramine, which strongly reduces circulating levels of FGF19 (the human ortholog of FGF15), induced CYP7A1 expression but not CYP8B1 (38, 39). Furthermore, repression of CYP7A1 by dietary bile acids was attenuated in livers of mice lacking βKlotho, an essential component of the FGF15 receptor complex, whereas CYP8B1 repression was not (40). Taken together with data in this study, these results demonstrate that the CYP7A1 gene is more responsive than CYP8B1 to repression by FGF15/19 emanating from the intestine. The molecular basis for this differential regulation and its physiological relevance remain to be determined.

In summary, liver-specific and intestine-specific *Fxr*-null mice were developed and used to demonstrate differential but complementary roles for FXR in liver and intestine in regulating bile acid homeostasis. This study provides the first direct evidence that FXR in intestine controls bile acid synthesis in liver and supports a previous hypothesis for intestine-produced FGF15 to regulate liver CYP7A1. Moreover, prominent differences were demonstrated in the mechanisms underlying feedback repression of CYP7A1 and CYP8B1. The tissue-specific *Fxr*-null mice will be powerful models for further investigation of the tissue-specific roles of FXR in bile acid metabolism and other physiologic and pathophysiologic processes.

This work was supported by National Institutes of Health National Cancer Institute Intramural Research Program, Grant DK-067158 (I.K., S-H.A., and S.I.), and the Robert A. Welch Foundation (S.A.K.). The authors thank Derek LeRoith and Deborah L. Gumucio for providing the albumin- and villin-cre

transgenic mouse lines, respectively, and Robert Gerard for help in preparing recombinant FGF15 protein.

REFERENCES

1. Hofmann, A. F. 1999. The continuing importance of bile acids in liver and intestinal disease. *Arch. Intern. Med.* **159:** 2647–2658.
2. Shaffer, E. A. 2000. Review article: control of gall-bladder motor function. *Aliment. Pharmacol. Ther.* **14:** 2–8.
3. Choi, M., A. Moschetta, A. L. Bookout, L. Peng, M. Umetani, S. R. Holmstrom, K. Suino-Powell, H. E. Xu, J. A. Richardson, R. D. Gerard, et al. 2006. Identification of a hormonal basis for gallbladder filling. *Nat. Med.* **12:** 1253–1255.
4. Krone, C. L. 1970. Defective intraluminal lipid digestion following ileectomy. *Ariz. Med.* **27:** 99–100.
5. Van Deest, B. W., J. S. Fordtran, S. G. Morawski, and J. D. Wilson. 1968. Bile salt and micellar fat concentration in proximal small bowel contents of ileectomy patients. *J. Clin. Invest.* **47:** 1314–1324.
6. Hofmann, A. F. 2002. Cholestatic liver disease: pathophysiology and therapeutic options. *Liver.* **22 (Suppl.):** 14–19.
7. Westergaard, H. 2007. Bile acid malabsorption. *Curr. Treat. Options Gastroenterol.* **10:** 28–33.
8. Claudel, T., E. Sturm, H. Duez, I. P. Torra, A. Sirvent, V. Kosykh, J. C. Fruchart, J. Dallongeville, D. W. Hum, F. Kuipers, et al. 2002. Bile acid-activated nuclear receptor FXR suppresses apolipoprotein A-I transcription via a negative FXR response element. *J. Clin. Invest.* **109:** 961–971.
9. Kast, H. R., C. M. Nguyen, C. J. Sinal, S. A. Jones, B. A. Laffitte, K. Reue, F. J. Gonzalez, T. M. Willson, and P. A. Edwards. 2001. Farnesoid X-activated receptor induces apolipoprotein C-II transcription: a molecular mechanism linking plasma triglyceride levels to bile acids. *Mol. Endocrinol.* **15:** 1720–1728.
10. Matsukuma, K. E., M. K. Bennett, J. Huang, L. Wang, G. Gil, and T. F. Osborne. 2006. Coordinated control of bile acids and lipogenesis through FXR-dependent regulation of fatty acid synthase. *J. Lipid Res.* **47:** 2754–2761.
11. Houten, S. M., M. Watanabe, and J. Auwerx. 2006. Endocrine functions of bile acids. *EMBO J.* **25:** 1419–1425.
12. Kim, I., K. Morimura, Y. Shah, Q. Yang, J. M. Ward, and F. J. Gonzalez. 2007. Spontaneous hepatocarcinogenesis in farnesoid X receptor-null mice. *Carcinogenesis.* **28:** 940–946.
13. Yang, F., X. Huang, T. Yi, Y. Yen, D. D. Moore, and W. Huang. 2007. Spontaneous development of liver tumors in the absence of the bile acid receptor farnesoid X receptor. *Cancer Res.* **67:** 863–867.
14. Huang, W., K. Ma, J. Zhang, M. Qatanani, J. Cuvillier, J. Liu, B. Dong, X. Huang, and D. D. Moore. 2006. Nuclear receptor-dependent bile acid signaling is required for normal liver regeneration. *Science.* **312:** 233–236.
15. Watanabe, M., S. M. Houten, C. Mataki, M. A. Christoffolete, B. W. Kim, H. Sato, N. Messaddeq, J. W. Harney, O. Ezaki, T. Kodama, et al. 2006. Bile acids induce energy expenditure by promoting intracellular thyroid hormone activation. *Nature.* **439:** 484–489.
16. Cariou, B., K. van Harmelen, D. Duran-Sandoval, T. H. van Dijk, A. Grefhorst, M. Abdelkarim, S. Caron, G. Torpier, J. C. Fruchart, F. J. Gonzalez, et al. 2006. The farnesoid X receptor modulates adiposity and peripheral insulin sensitivity in mice. *J. Biol. Chem.* **281:** 11039–11049.
17. Ma, K., P. K. Saha, L. Chan, and D. D. Moore. 2006. Farnesoid X receptor is essential for normal glucose homeostasis. *J. Clin. Invest.* **116:** 1102–1109.
18. Zhang, Y., F. Y. Lee, G. Barrera, H. Lee, C. Vales, F. J. Gonzalez, T. M. Willson, and P. A. Edwards. 2006. Activation of the nuclear receptor FXR improves hyperglycemia and hyperlipidemia in diabetic mice. *Proc. Natl. Acad. Sci. USA.* **103:** 1006–1011.
19. Bilz, S., V. Samuel, K. Morino, D. Savage, C. S. Choi, and G. I. Shulman. 2006. Activation of the farnesoid X receptor improves lipid metabolism in combined hyperlipidemic hamsters. *Am. J. Physiol. Endocrinol. Metab.* **290:** E716–E722.
20. Goodwin, B., S. A. Jones, R. R. Price, M. A. Watson, D. D. McKee, L. B. Moore, C. Galardi, J. G. Wilson, M. C. Lewis, M. E. Roth, et al. 2000. A regulatory cascade of the nuclear receptors FXR, SHP-1, and LRH-1 represses bile acid biosynthesis. *Mol. Cell.* **6:** 517–526.
21. Lu, T. T., M. Makishima, J. J. Repa, K. Schoonjans, T. A. Kerr, J. Auwerx, and D. J. Mangelsdorf. 2000. Molecular basis for feedback regulation of bile acid synthesis by nuclear receptors. *Cell.* **6:** 507–515.
22. Lee, H., Y. Zhang, F. Y. Lee, S. F. Nelson, F. J. Gonzalez, and P. A. Edwards. 2006. FXR regulates organic solute transporters alpha and beta in the adrenal gland, kidney, and intestine. *J. Lipid Res.* **47:** 201–214.
23. Ananthanarayanan, M., N. Balasubramanian, M. Makishima, D. J. Mangelsdorf, and F. J. Suchy. 2001. Human bile salt export pump promoter is transactivated by the farnesoid X receptor/bile acid receptor. *J. Biol. Chem.* **276:** 28857–28865.
24. Plass, J. R., O. Mol, J. Heegsma, M. Geuken, K. N. Faber, P. L. Jansen, and M. Muller. 2002. Farnesoid X receptor and bile salts are involved in transcriptional regulation of the gene encoding the human bile salt export pump. *Hepatology.* **35:** 589–596.
25. Landrier, J. F., J. J. Eloranta, S. R. Vavricka, and G. A. Kullak-Ublick. 2006. The nuclear receptor for bile acids, FXR, transactivates human organic solute transporter-alpha and -beta genes. *Am. J. Physiol. Gastrointest. Liver Physiol.* **290:** G476–G485.
26. Sinal, C. J., M. Tohkin, M. Miyata, J. M. Ward, G. Lambert, and F. J. Gonzalez. 2000. Targeted disruption of the nuclear receptor FXR/BAR impairs bile acid and lipid homeostasis. *Cell.* **102:** 731–744.
27. Guo, G. L., G. Lambert, M. Negishi, J. M. Ward, H. B. Brewer, Jr., S. A. Kliewer, F. J. Gonzalez, and C. J. Sinal. 2003. Complementary roles of farnesoid X receptor, pregnane X receptor, and constitutive androstane receptor in protection against bile acid toxicity. *J. Biol. Chem.* **278:** 45062–45071.
28. Holt, J. A., G. Luo, A. N. Billin, J. Bisi, Y. Y. McNeill, K. F. Kozarsky, M. Donahee, D. Y. Wang, T. A. Mansfield, S. A. Kliewer, et al. 2003. Definition of a novel growth factor-dependent signal cascade for the suppression of bile acid biosynthesis. *Genes Dev.* **17:** 1581–1591.
29. Inagaki, T., M. Choi, A. Moschetta, L. Peng, C. L. Cummins, J. G. McDonald, G. Luo, S. A. Jones, B. Goodwin, J. A. Richardson, et al. 2005. Fibroblast growth factor 15 functions as an enterohepatic signal to regulate bile acid homeostasis. *Cell Metab.* **2:** 217–225.
30. Liu, J. L., A. Grinberg, H. Westphal, B. Sauer, D. Accili, M. Karas, and D. LeRoith. 1998. Insulin-like growth factor-I affects perinatal lethality and postnatal development in a gene dosage-dependent manner: manipulation using the Cre/loxP system in transgenic mice. *Mol. Endocrinol.* **12:** 1452–1462.
31. Madison, B. B., L. Dunbar, X. T. Qiao, K. Braunstein, E. Braunstein, and D. L. Gumucio. 2002. Cis elements of the villin gene control expression in restricted domains of the vertical (crypt) and horizontal (duodenum, cecum) axes of the intestine. *J. Biol. Chem.* **277:** 33275–33283.
32. Hayhurst, G. P., Y. H. Lee, G. Lambert, J. M. Ward, and F. J. Gonzalez. 2001. Hepatocyte nuclear factor 4alpha (nuclear receptor 2A1) is essential for maintenance of hepatic gene expression and lipid homeostasis. *Mol. Cell. Biol.* **21:** 1393–1403.
33. Inoue, Y., A. M. Yu, J. Inoue, and F. J. Gonzalez. 2004. Hepatic nuclear factor 4alpha is a central regulator of bile acid conjugation. *J. Biol. Chem.* **279:** 2480–2489.
34. Kok, T., C. V. Hulzebos, H. Wolters, R. Havinga, L. B. Agellon, F. Stellaard, B. Shan, M. Schwarz, and F. Kuipers. 2003. Enterohepatic circulation of bile salts in farnesoid X receptor-deficient mice: efficient intestinal bile salt absorption in the absence of ileal bile acid-binding protein. *J. Biol. Chem.* **278:** 41930–41937.
35. Gutierrez, A., E. P. Ratliff, A. M. Andres, X. Huang, W. L. McKeehan, and R. A. Davis. 2006. Bile acids decrease hepatic paraoxonase 1 expression and plasma high-density lipoprotein levels via FXR-mediated signaling of FGFR4. *Arterioscler. Thromb. Vasc. Biol.* **26:** 301–306.
36. Shih, D. M., H. R. Kast-Woelbern, J. Wong, Y. R. Xia, P. A. Edwards, and A. J. Lusis. 2006. A role for FXR and human FGF-19 in the repression of paraoxonase-1 gene expression by bile acids. *J. Lipid Res.* **47:** 384–392.
37. Wang, L., Y. K. Lee, D. Bundman, Y. Han, S. Thevananther, C. S. Kim, S. S. Chua, P. Wei, R. A. Heyman, M. Karin, et al. 2002. Redundant pathways for negative feedback regulation of bile acid production. *Dev. Cell.* **2:** 721–731.
38. Abrahamsson, A., U. Gustafsson, E. Ellis, L. M. Nilsson, S. Sahlin, I. Bjorkhem, and C. Einarsson. 2005. Feedback regulation of bile acid synthesis in human liver: importance of HNF-4alpha for regulation of CYP7A1. *Biochem. Biophys. Res. Commun.* **330:** 395–399.
39. Lundasen, T., C. Galman, B. Angelin, and M. Rudling. 2006. Circulating intestinal fibroblast growth factor 19 has a pronounced diurnal variation and modulates hepatic bile acid synthesis in man. *J. Intern. Med.* **260:** 530–536.
40. Ito, S., T. Fujimori, A. Furuya, J. Satoh, Y. Nabeshima, and Y. Nabeshima. 2005. Impaired negative feedback suppression of bile acid synthesis in mice lacking betaKlotho. *J. Clin. Invest.* **115:** 2202–2208.